

pubs.acs.org/JPCC Article

Probing the Properties of Pt-Cu(111) Bimetallic Surfaces with Adsorbed CO

David L. Molina, Maki Inagaki, Emiko Kazuma, Yousoo Kim, and Michael Trenary*



Cite This: J. Phys. Chem. C 2023, 127, 9796-9806



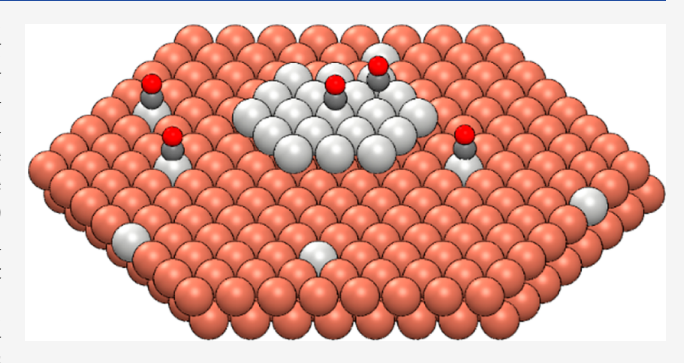
ACCESS I

III Metrics & More

Article Recommendations

s Supporting Information

ABSTRACT: Reflection absorption infrared spectroscopy and temperature-programmed desorption of adsorbed CO were used to probe the properties of Pt/Cu(111) surfaces. For Pt deposition on Cu(111) at room temperature, the Pt coverage was varied from a multilayer film to 0.23 monolayer (ML). As the Pt coverage decreased, isolated Pt atoms embedded in the Cu(111) surface were revealed by a C-O stretch peak in the range of 2041–2050 cm⁻¹. The presence of Pt islands was indicated by a C-O stretch peak in the range of 2058–2067 cm⁻¹ accompanied by a peak at 1852 cm⁻¹ due to a CO bridge-bonded between two Pt atoms. Deposition of low coverages of Pt at 380, 450, and 550 K formed single atom alloys (SAAs) in which surface Pt is only present as



isolated atoms that had replaced Cu atoms in the topmost atomic layer, in agreement with previous studies with scanning tunneling microscopy. Adsorption of CO on top of the Pt atoms of the SAAs leads to a C-O stretch in the range of 2041–2046 cm⁻¹. Compared to the SAAs formed by Pt deposition at 380 K, deposition at 450 and 550 K led to more dispersed Pt atoms, as indicated by the lack of a shift of the C-O stretch peaks, indicating that the distance between CO molecules was not low enough for dipole—dipole coupling shifts to occur. In all cases, the C-O stretch of CO on the Pt atoms of Pt/Cu(111) was significantly red-shifted relative to its value on Pt(111), which is a manifestation of how nearby Cu atoms alter the Pt-CO bonding.

1. INTRODUCTION

The structure and properties of bimetallic surfaces are of great interest for a variety of reasons, including the use of bimetallic catalysts for various industrial processes. 1,2 For this reason, Pt films deposited onto the Cu(111) surface have been subjected to several studies. The surface properties of the Cu₃Pt(111) surface have also been studied. 3,4 One way to characterize bimetallic surfaces is through infrared (IR) studies of adsorbed CO. Because the C-O stretch frequency is a sensitive indicator of the adsorption site, it is straightforward to determine if CO is adsorbed at atop, 2-fold bridge, or 3-fold hollow sites, which can provide information on the type of adsorption sites available. The value of the C-O stretch for a given adsorption site can also provide information about the nature of the metal-CO bond. Because of the high intensity of the C-O stretch peak, IR spectroscopy of adsorbed CO can be used to probe the properties of metal atoms present at very low surface coverages. Here we have used reflection absorption infrared spectroscopy (RAIRS) along with temperatureprogrammed desorption (TPD) to probe the properties of the Pt/Cu(111) system from multilayer films to the single atom alloy (SAA) limit, where isolated Pt atoms replace Cu atoms in the topmost atomic layer.⁶ Previous work has shown that RAIRS of adsorbed CO is a particularly powerful way to probe the surface properties of the active metal in SAAs.⁷ Despite the extensive prior studies of the Pt/Cu(111) system,

it has not been previously characterized using RAIRS of adsorbed CO. By interpreting the new results presented here in the context of what has been learned from previous studies with complementary techniques, we have gained new insights into this system.

Three previous studies have used low energy electron diffraction (LEED) to show that the same (1×1) pattern is obtained for clean Cu(111) and for 1 ML of Pt deposited at room temperature. After approximately 5 MLs of Pt were deposited, the LEED spots shifted to those of the Pt(111) surface. In addition, Fusy et al. used reflection high energy electron diffraction (RHEED) to show that the Pt–Pt distance was 2.55 Å (the Cu–Cu distance for Cu(111)) for 1 ML of Pt and continually evolved to 2.75 Å for 6.5 ML of Pt, just short of the 2.77 Å expected for Pt(111). These results demonstrate that the first Pt layer grows epitaxially to produce a pseudomorphic Pt layer that is compressed to match the Cu(111) lattice. Belkhou et al. also used Auger electron

Received: February 8, 2023 Revised: April 25, 2023 Published: May 15, 2023





spectroscopy (AES) to show that Pt thin films deposited onto a Cu(111) surface grow layer-by-layer up to 3 monolayers and from X-ray photoelectron diffraction found that the Pt layers have a face-centered cubic (fcc) structure. 10 In further work, Belkhou showed that annealing Pt on Cu(111) to higher temperatures led to alloy formation.¹⁴ Shen et al. used low energy Li⁺ ion scattering to show that Pt layers grow epitaxially on Cu(111) at room temperature and that upon annealing the Pt layers to 300 °C, a Cu₃Pt(111) alloy was formed.¹¹ From TPD studies of adsorbed CO and Xe and high resolution electron energy loss spectroscopy (HREELS) of adsorbed CO, Schröder et al. found that annealing a Pt/Cu(111) surface to 500 K resulted in Pt atoms dispersed in the topmost Cu layer. 15 Fusy et al. used AES and RHEED to also conclude that Pt grows layer-by-layer, with no difference in growth mode for substrate temperatures of 100 and 300 K.¹³ They also used TPD of adsorbed CO as well as photoemission of adsorbed Xe (PAX) to probe the properties of Pt/Cu(111).¹³ They noted that while a monolayer of Pt yielded CO TPD results similar to those of Pt(111), the PAX results indicated that the electronic properties of the Pt were modified through interaction with the underlying Cu layer. 13

Lucci et al. investigated the atomic-scale properties of low coverages (0.01 to 0.1 ML) of Pt deposited onto Cu(111) held at 315, 450, and 550 K with scanning tunneling microscopy (STM) at 30 and 300 K.16 They found intermixing of Pt and Cu to form alloys even for deposition at 315 K. At 315 K, the Pt directly replaced Cu atoms in the (111) terraces and accumulated at step edges through a site exchange mechanism. For deposition at 550 K, the Pt was mainly found dispersed in the (111) terraces with little accumulation at the steps. It was possible to not only distinguish Pt from Cu atoms in the surface layer with STM but also to distinguish surface Cu atoms above subsurface Pt atoms. It was found that, for deposition temperatures of 315, 450, and 550 K, 99, 70, and 20% of the Pt, respectively, was in the topmost atomic layer of the Cu(111) surface. 16 At the higher Pt coverage of 0.1 ML, deposition at 315 K produced both islands and fingers that grew out of the step edges. The fingers and islands contained both Pt and Cu, with Pt atoms more prevalent at the edges of the islands. These results demonstrate that the actual structures formed when Pt is deposited on Cu(111) are considerably more complicated than might be implied by simple layer-by-layer epitaxial growth. In a subsequent publication, Lucci et al. showed that a low coverage of Pt deposited onto Cu(111) at 380 K gave well dispersed Pt atoms substituted into the topmost Cu layer.¹⁷ We have therefore used a deposition temperature of 380 K to prepare the Pt/ Cu(111) SAA.

The interpretation of our RAIRS results for CO adsorbed on Pt/Cu(111) is aided by the extensive previous RAIRS work for CO on both Pt(111) and Cu(111). These previous studies have shown that CO adsorbs at the atop sites first on both surfaces, followed by occupation of higher coordination sites at higher coverages. In the case of CO on Cu(111), the atop site frequency red-shifts from 2078 cm $^{-1}$ at lower coverages to 2068 cm $^{-1}$ at saturation. The red-shift is due to a negative chemical shift being larger than the positive dipole—dipole coupling shift, which is absent in the limit of zero coverage. Persson and Liebsch 19 extrapolated the experimental isotopic dilution data of Hollins and Pritchard 18 to conclude that in the absence of coupling, the C–O stretch of CO on Cu(111) at a coverage of 1/3 ML for the $(\sqrt{3}\times\sqrt{3})$ –R 30° structure

would be 2046 cm⁻¹. On a Pt(111) surface with few defects, the CO atop frequency blue-shifts from 2089 cm⁻¹ at low coverages to 2103 cm⁻¹ at saturation.²⁰ The large blue-shift is the net result of the positive dipole—dipole coupling shift being larger than the negative chemical shift. 20-22 Tüshaus et al. estimated a frequency of 2078 cm⁻¹ for a single ¹²C¹⁶O molecule surrounded by 12C18O molecules at a total CO coverage of 0.3 ML.²⁰ For CO at step sites and defect sites on a Pt(111) surface, the C-O stretch has been observed in the range of 2057–2072 cm⁻¹. ^{20,23,24} Correlations between RAIR spectra and the overlayer structures observed with LEED have been established not only for the C-O stretch^{20,22,25} but also for the Pt-CO stretch. 26,27 In addition to inferences about ordered CO structures from RAIRS and LEED studies, direct observations of these structures have been made with molecule-resolved STM images.²⁸ Although there is some overlap in the range of C-O stretch frequencies for atop CO on Pt(111) and Cu(111), CO desorbs from the two surfaces in widely separated temperature ranges; depending on coverage, CO desorbs from Pt(111) in the range of 350-550 K,²¹ whereas CO desorbs from Cu(111) from 120 to 180 K.³⁰ For this reason, CO is expected to adsorb only on Pt sites at room temperature, which allows unambiguous assignment of C-O stretch peaks for CO adsorbed on Pt versus Cu sites.

An additional motivation for studying the interaction of CO with Pt/Cu(111) is to address the problem of CO poisoning of Pt catalysts. If alloying Pt with Cu can reduce the strength of the CO-Pt interaction without significantly reducing the catalytic activity of the Pt, then this would be a viable strategy for developing catalysts that are resistant to CO poisoning. To address the ability of SAAs to mitigate CO poisoning, Darby et al. carried out a comprehensive theoretical study of CO interaction with highly dilute alloys of the platinum group metals Pd, Pt, Rh, Ir, and Ni with the coinage metal hosts Cu, Ag, and Au. 31 Included in their study were calculations of the C-O stretch frequency for CO at the atop sites of Pt in a Cu(111) host, to which our experimental results can be directly compared. In a study similar to ours, Liu et al. presented CO TPD results for various coverages of Pt on Cu(111) as well as IR results for nanoparticles of Pt, Cu, a Pt_{0.39}Cu alloy, and a Pt_{0.008}Cu SAA supported on Al₂O₃. The RAIRS results presented here differ substantially from the IR spectra of Liu et al.³² This difference suggests a significant influence of the Al₂O₃ support in the interaction of CO with the nanocatalyst SAA that is absent in the Pt/Cu(111) SAA.

2. EXPERIMENTAL SECTION

The experiments were carried out at the University of Illinois Chicago in an ultrahigh vacuum (UHV) chamber with a base pressure of 2×10^{-10} Torr. The chamber is equipped with a PHI 10-115 cylindrical mirror analyzer for AES, PHI 15-120 optics for LEED, and a Hiden HAL201/3F quadrupole mass spectrometer for TPD. The UHV chamber is coupled to a Bruker IFS-66v/s Fourier transform infrared (FTIR) spectrometer. The incident and reflected IR beams enter and exit the UHV chamber through differentially pumped, O-ring sealed NaCl and KBr windows. Pressures were measured with a Bayard–Alpert hot filament ion gauge.

The copper single crystal from Surface Preparation Laboratory is circular with a diameter of 15 mm and a thickness of 2.5 mm with a (111) orientation (<0.1° accuracy). It is mounted by passing two tungsten wires through holes (0.75 mm diameter) parallel to the (111) face on opposite

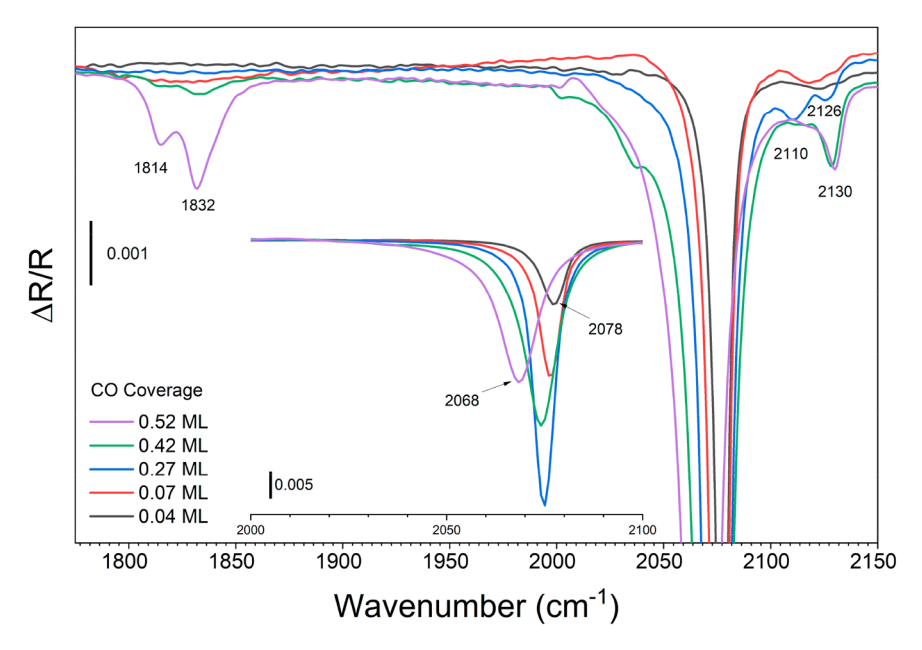


Figure 1. RAIR spectra versus CO coverage on the clean Cu(111) surface at 90 K. The inset shows the atop CO stretch that red-shifts from 2078 to 2068 cm⁻¹ as the coverage increases. The spectrum at 0.52 ML shows peaks due to physisorbed CO at 2130 cm⁻¹ and bridge-bonded CO at 1814 and 1832 cm⁻¹.

edges of the crystal. A K-type thermocouple junction is inserted into a hole in the top edge of the crystal (0.3 mm in diameter with a depth of 0.8 mm). The crystal was cleaned with Ar sputtering (1 keV, 7 μ A) cycles and annealing at 900 K. The cleanness of the crystal was determined using AES and RAIRS of CO. The absence of a RAIRS peak at 300 K for CO on Pt sites confirmed the absence of platinum below the AES detection limit.

A commercial electron-beam evaporator (EBE35A ACME) was used to deposit Pt onto the Cu(111) surface at 300 K with a background pressure at 1×10^{-9} Torr. The AES spectra were taken after the pressure was below 9×10^{-10} Torr. Except where otherwise noted, all RAIR spectra were obtained at room temperature by the following procedure. After obtaining Auger spectra, the crystal was annealed at 400 K for 1 min and allowed to cool to room temperature. The RAIR reference spectrum was taken, and a series of CO exposures were made until the RAIRS intensity showed no change. The crystal was then cooled to 90 K, subsequently annealed at 200 K, and exposed to an additional 2 L of CO to saturate the surface at 200 K given that the absolute coverages of CO on Pt(111) at room temperature and 210 K have been shown to be 0.50 and 0.60 ML respectively.²⁵ CO coverages for different Pt coverages are referenced to these values. The crystal was then cooled to 90 K, and the TPD spectrum was obtained (90-575 K). The intensity scale for the TPD plots is the CO partial pressure in Torr based on the sensitivity of the mass spectrometer, which although based on N2 should be essentially the same for CO as the two molecules have almost the same electron impact ionization cross sections. The CO TPD area of the Pt film on Cu(111), where the Cu AES signal was not observed, was used to calculate Pt coverages of other Pt/Cu alloys given that background noise and weak Pt signals made coverage estimates from AES unreliable. The SAA surfaces were prepared with the Cu(111) crystal kept at 380, 450, or 550 K during Pt deposition.

An ion flux of $\sim 5.4 \times 10^9$ Pt ions/s was measured at the crystal surface (RBD 9103 Autoranging Picoammeter) for deposition above the SAA range. The ion flux is a small portion of the actual flux, consisting mostly of neutrals, which are not measured. A lower flux was used for the SAAs. The Pt rod (99.99%) was obtained from ESPI Metals. RAIR spectra were collected with 1024 scans, 4 cm⁻¹ resolution, and are presented without baseline correction. A linear rate of 0.5 K/s was used to obtain the TPD data, which were smoothed. The CO (99.99%) was obtained from Matheson and used without further purification.

3. RESULTS

Our RAIRS results for CO adsorption on Cu(111) at 90 K are consistent with previous studies. 18,33-36 Figure 1 shows the RAIR spectra of CO as a function of coverage, with the saturation coverage previously estimated as 0.52 ML at this temperature. 18 The inset shows that the frequency for atop CO first appears at 2078 cm⁻¹ and red-shifts to 2068 cm⁻ coverage increases. The enlarged full spectrum shows the bridge site peaks at 1814 and 1832 cm⁻¹, and CO stretches at 2110 cm⁻¹ and 2126–2130 cm⁻¹ assigned to physisorbed CO. The intensity of the physisorbed CO peaks seen here relative to the atop peak is vastly lower than seen previously only for T \leq 25 K. ^{33,35,36} Given the signal-to-noise ratios in the previous studies, physisorbed CO peaks of such low intensity would not have been observable. 33,35,36 The peaks of the physisorbed species first appear at 2110 cm⁻¹ and shift to 2126 cm⁻¹ by 0.27 ML, while the peaks of the bridge species first appear at 0.42 ML. These observations are consistent with the mechanism proposed by Eve et al., where the physisorbed species appear first and are compressed into a moderately stable bridge site species. 35,36 Although bridge-bonded CO on Cu(111) was not detected by Hollins and Pritchard, they noted that changes in the peak width for the atop CO changed as the overlayer structures detected with LEED changed. The TPD results in Figure 2 for an initial CO coverage of 0.52 ML

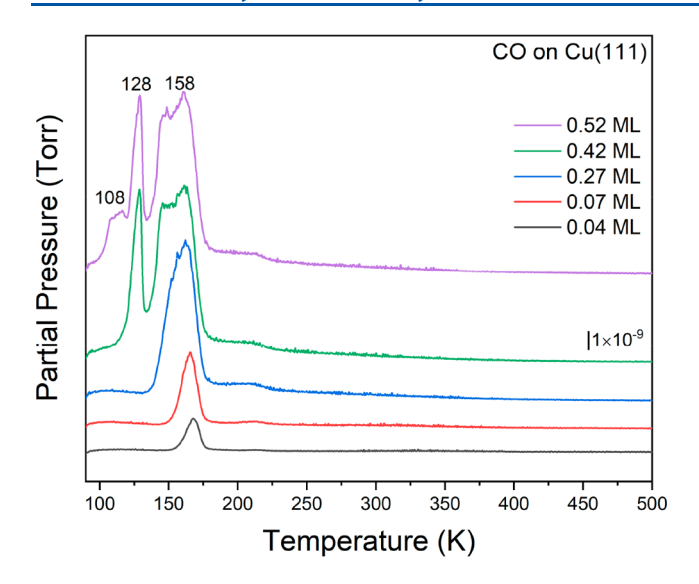


Figure 2. TPD of CO on Cu(111) versus CO coverage after adsorption at 90 K.

at 90 K on clean Cu(111) are in rough agreement with those of Kirstein et al.³⁰ and show that CO desorbs as three peaks at 108, 128, and 158 K. Figure 3 shows RAIR spectra after

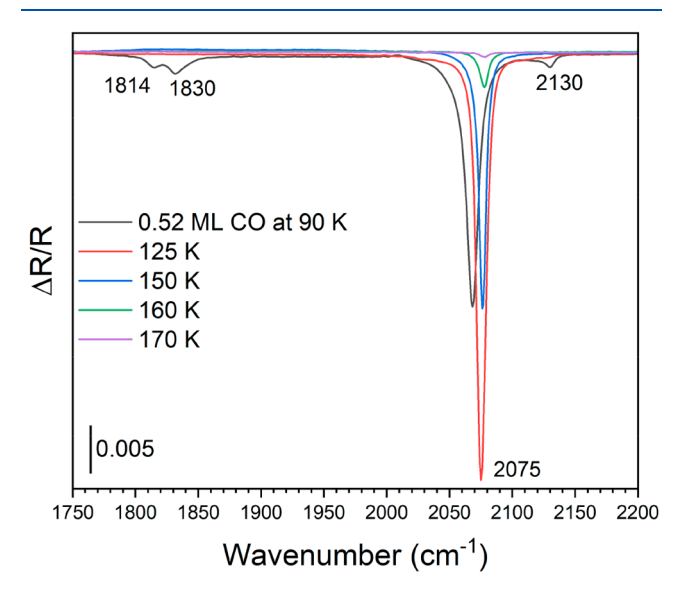


Figure 3. RAIR spectra after adsorption of a saturation coverage of 0.52 ML of CO on the clean Cu(111) surface at 90 K and after annealing to the indicated temperatures. The bands of the bridge and physisorbed species are not present after the 125 K anneal.

adsorption of 0.52 ML of CO at 90 K on Cu(111) and annealing to the indicated temperatures. Comparison with the TPD results of Figure 2 indicates that annealing at 125 K leads to the loss of the bridge site and physisorbed CO, leaving a single sharp and intense peak at 2075 cm $^{-1}$, which other studies have shown corresponds to the $(\sqrt{3}\times\sqrt{3})-R$ 30° structure. 18

Figure 4 shows AES spectra after depositing Pt on the Cu(111) surface at 300 K. In the yellow spectrum, Cu peaks are barely visible, implying that it corresponds to a Pt film only a few layers thick. Pt growth on Cu(111) has been shown to follow a layer-by-layer growth mode at 300 K, where quasiepitaxial growth is seen for coverages below 2 ML and

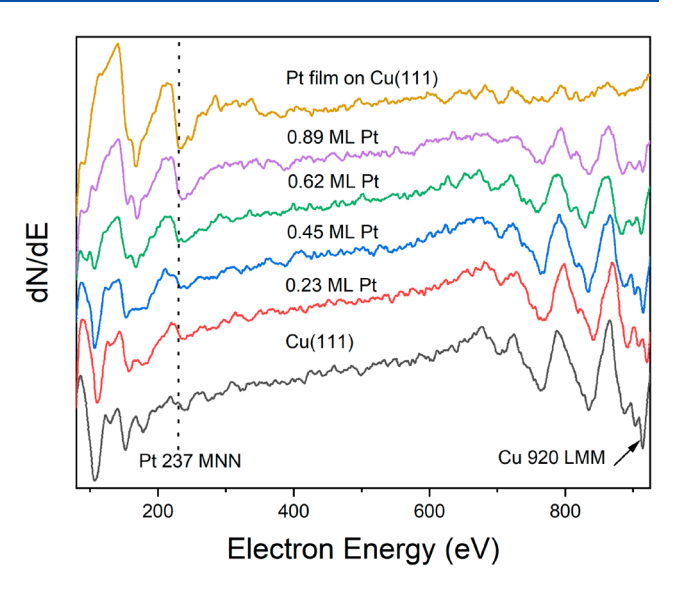


Figure 4. AES spectra for different Pt coverages on Cu(111) at 300 K. The Pt 237 MNN and Cu 920 LMM transitions are marked. The Pt coverages were calculated from the CO TPD results as described in the text.

coverages close to 5 ML resemble the Pt(111) surface. 10,12,13 We assume that this is a pseudomorphic film, meaning that the lattice constant has not fully relaxed from that of Cu(111) to that of Pt(111). Figure 5a shows the TPD results after a saturation CO exposure at 200 K to a multilayer Pt film, assumed to correspond to a CO coverage of 0.60 ML, which is the saturation CO coverage at 210 K on Pt(111).²⁵ By fitting the overall CO TPD trace to separate peaks, the peak areas for CO desorbing from Pt sites were obtained. The CO peak areas associated with Pt for subsequent TPD results were then used to obtain both Pt and CO coverages based on the assumption of a saturation CO coverage of 0.60 ML for multilayer Pt films. Thus, lower CO saturation coverages were attributed to Pt coverages of less than one monolayer. For Figures 5-8, Pt was also deposited at 300 K. The TPD results in Figure 5a closely resemble what is seen for a saturation coverage of CO at 210 K on the Pt(111) surface. 25,29,37,38 The presence of at least two peaks in the TPD results for a saturation coverage of CO on the Pt multilayer, and on lower coverages of Pt, are similar to what is seen from Pt(111) and is attributed to CO-CO interactions at higher coverages, which lowers the binding energy of the CO. As the CO coverage is reduced during the TPD run, the remaining CO is more strongly bound to the surface and desorbs at the high temperatures seen for a very low initial CO coverage. Despite the lack of a Cu AES signal, Figure 5a shows that desorption starts as low as 200 K, which is attributed to gaps in the Pt layer that allow CO to penetrate to the Cu surface.

Figure 5b shows the CO RAIR spectra at 300 K of the same Pt film for CO coverages from 0.033 ML (black) to 0.50 ML (orange). At 0.50 ML, there are three distinct peaks at 1862, 2065, and 2089 cm⁻¹. The 1862 cm⁻¹ peak is due to CO at 2-fold Pt bridge sites.²⁵ The peak at 2089 cm⁻¹ corresponds to CO on top of Pt atoms, and its blue-shift with increasing coverage is consistent with previous RAIRS results for CO adsorption on Pt(111) at 300 K.^{20,21,25} At the lowest coverage (black spectrum), the positive-pointing peak is at 2065 cm⁻¹. This peak can be plausibly assigned to either CO on top of Pt atoms at defect sites²⁰ or to CO at low coverage on terrace

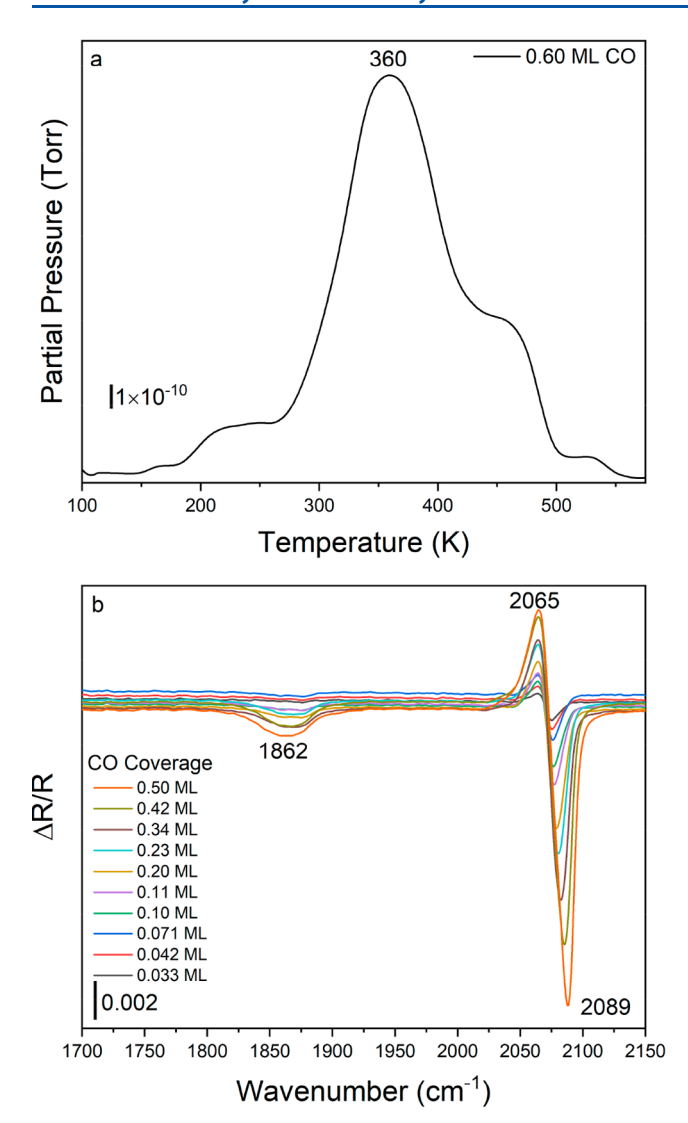


Figure 5. (a) CO TPD from a multilayer Pt film on Cu(111) with a peak maximum at 360 K. The surface was saturated at 200 K (0.60 ML). (b) RAIR spectra following CO adsorption at room temperature showing peaks for CO at bridge sites (1862 cm⁻¹) and atop sites (2065–2089 cm⁻¹). The positive peak at 2065 cm⁻¹ is attributed to CO from the background that was present on the surface when the reference spectrum was obtained. As the CO coverage increased, the C–O stretch frequency increased, causing less cancellation of the 2065 cm⁻¹ peak. This accounts for the growth of this peak at constant frequency as the coverage increased.

sites. In either case, this peak points upward due to CO that had adsorbed from the chamber background when the reference spectrum of the nominally clean surface was obtained. As noted by Hayden and Bradshaw, ²⁵ the peak due to atop CO for adsorption at 300 K on Pt(111) shifts from 2068 to 2086 cm⁻¹ from lowest to highest coverages. As CO coverage increases, the shift in the peak position leads to less cancellation of the peak at 2065 cm⁻¹, leading to its apparent increase in intensity with increasing CO coverage. There may also be some shift of CO from defect sites to terrace sites or a transfer of intensity from the defect site CO to the terrace site CO molecules due to dipole—dipole coupling. ³⁹ Any of these effects or some combination of them can be the origin of the 2065 cm⁻¹ peak. The relatively high amount of CO on the surface in the reference spectrum is because the surface was

annealed to only 400 K to avoid diffusion of Pt into the subsurface of the copper crystal. $^{11,14-16,40}$ This is not a high enough temperature to desorb the CO that had adsorbed from the background. As shown below, for lower Pt coverages there is less of a blue-shift of the C–O stretch, so the positive peak on the low wavenumber side of the main peak decreases due to more complete cancellation in the ratio spectrum. For the SAA surface, there is no shift in the C–O stretch with coverage, and consequently there is no positive low-wavenumber component to the C–O stretch peak.

Figure 6a shows the TPD results for 0.53 ML of CO deposited at 200 K on a 0.89 ML Pt/Cu(111) surface. The

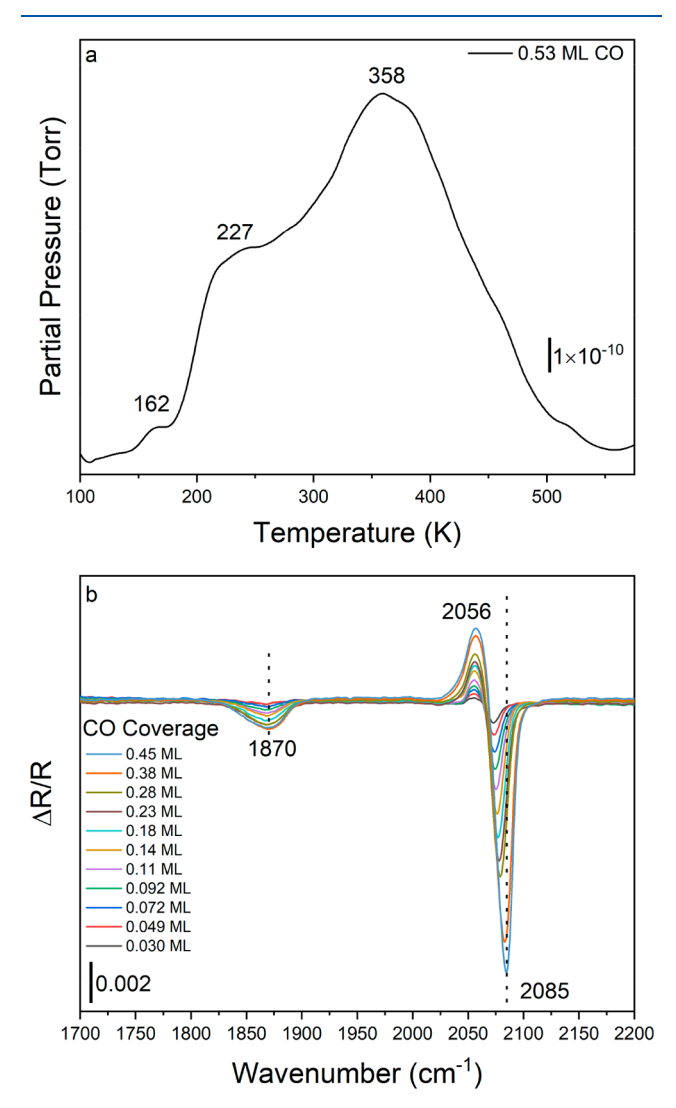
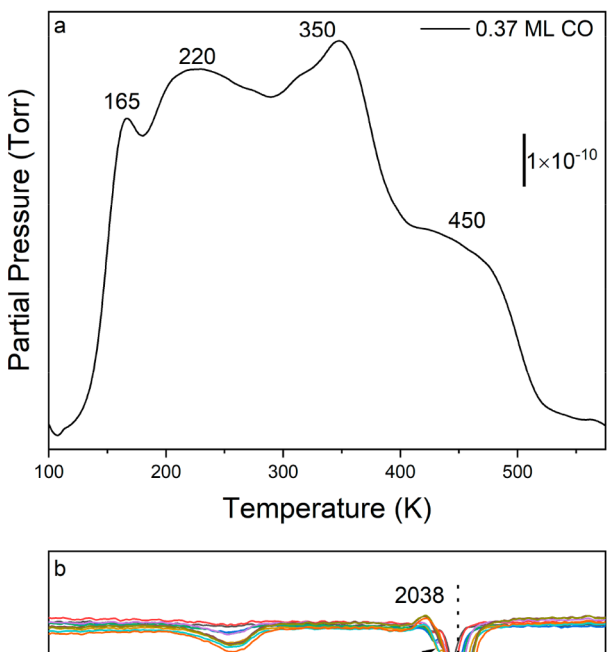


Figure 6. (a) CO TPD for a 0.89 ML Pt/Cu(111) surface showing CO desorption at 227 and 358 K. The surface was saturated at 200 K (0.53 ML). (b) Room temperature RAIR spectra versus CO coverage show the bands for CO at bridge sites and atop sites at 1870 and 2056–2085 cm⁻¹, respectively. As for Figure 5b, the origin of the 2056 cm⁻¹ peak is CO from the background that was on the surface when the reference spectrum was acquired.

three desorption peaks are at similar temperatures as seen by Fusy et al. for 0.8 ML of Pt on Cu(111). These can be associated with CO desorbing from Cu sites (162 K), mixed Cu–Pt sites (227 K), and Pt sites (358 K). A small shoulder can also be observed above 400 K. For the same 0.89 ML Pt/

Cu(111) surface, Figure 6b shows RAIR spectra for CO coverages ranging from 0.030 to 0.45 ML at 300 K. Similar to the results of Figure 5b, peaks are seen for the bridge and atop sites of Pt islands at 1870 and 2085 cm⁻¹, respectively. The positive-pointing peak at 2056 cm⁻¹ has the same origin as the 2065 cm⁻¹ peak in Figure 5b.

Figure 7a shows the TPD results for 0.37 ML of CO deposited at 200 K on a 0.62 ML Pt/Cu(111) surface. The



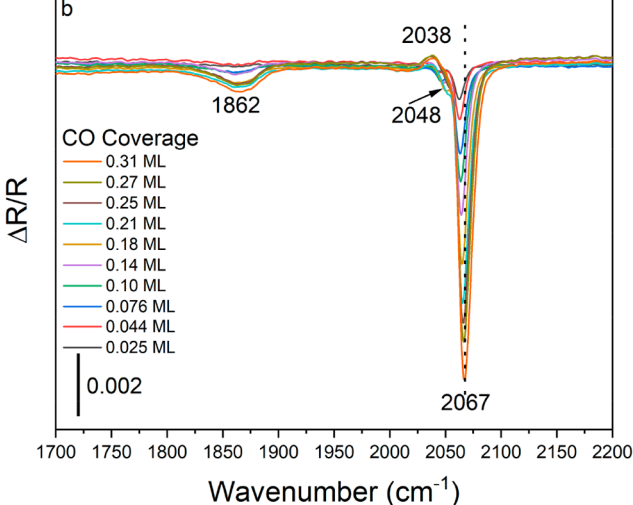
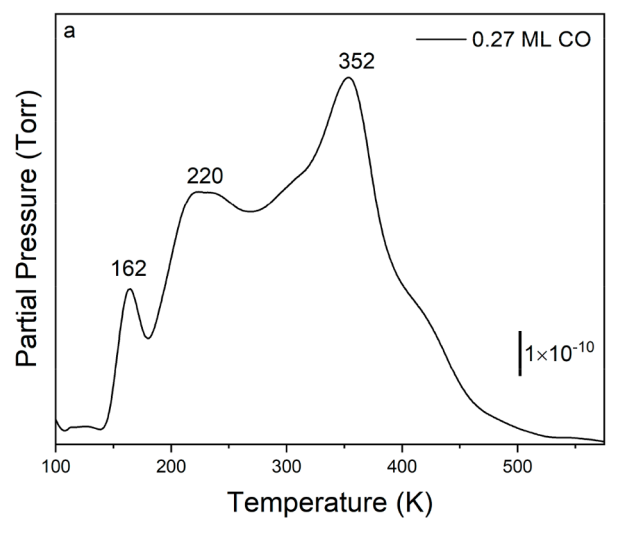


Figure 7. (a) CO TPD from a 0.62 ML Pt/Cu(111) surface showing peaks at 165, 220, 350, and 450 K. The surface was saturated at 200 K (0.37 ML). (b) Room temperature RAIR spectra showing bands for CO at bridge sites ($1862~{\rm cm}^{-1}$) and atop sites ($2067~{\rm cm}^{-1}$) of Pt islands. The small peak at 2048 cm $^{-1}$ is assigned to CO on an isolated Pt atom embedded in the topmost atomic layer of the Cu(111) surface. The small positive peak 2038 cm $^{-1}$ is attributed to CO from the background that was on the surface when the reference spectrum was obtained.

TPD trace is slightly more complicated with four desorption peaks attributed to CO on Cu sites, CO on mixed Cu–Pt sites, and two peaks for CO on Pt sites at 162, 220, 350, and 450 K, respectively. Figure 7b shows the complementary RAIR spectra for the 0.62 ML Pt/Cu(111) surface for CO coverages ranging from 0.025 to 0.31 ML. The main peak reaches a final value of 2067 cm⁻¹ at the highest CO coverage of 0.31 ML after

undergoing a very small shift from 2062 cm⁻¹ at the lowest CO coverage of 0.025 ML. This small shift is most likely associated with CO adsorbed on smaller Pt islands, where the full effect of the long-range dipole—dipole coupling shift cannot occur. The presence of small Pt aggregates, as opposed to isolated Pt atoms, is revealed by the peak at 1862 cm⁻¹ due to CO on 2-fold Pt bridge sites. A positive peak at 2038 cm⁻¹ due to CO on the surface when the reference spectrum was obtained is visible at the highest CO coverages. A shoulder at 2048 cm⁻¹ is visible at intermediate coverages and is most distinct at 0.21 ML. As the results described below indicate, this peak is associated with CO on isolated Pt atoms surrounded by Cu atoms.

Figure 8a shows TPD results for 0.27 ML CO deposited at 200 K on a 0.45 ML Pt/Cu(111) surface. CO desorbs from Cu, mixed Cu–Pt, and Pt sites at 162, 220, and 352 K, respectively. Comparing Figures 7a and 8a indicates that contrary to expectation, the peak associated with CO desorption from Cu sites is larger at the higher Pt coverage



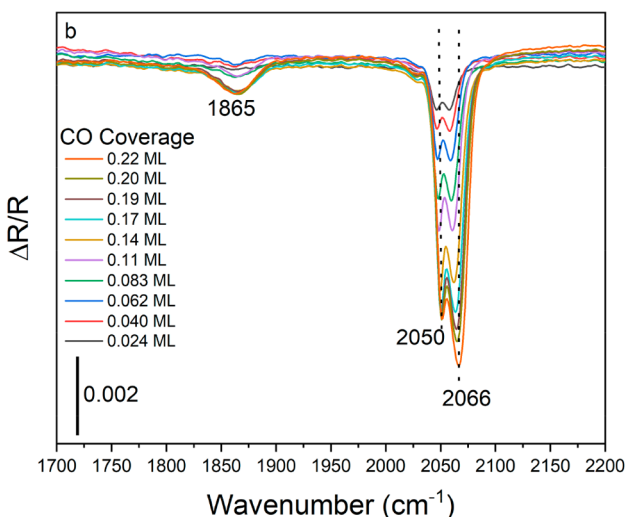


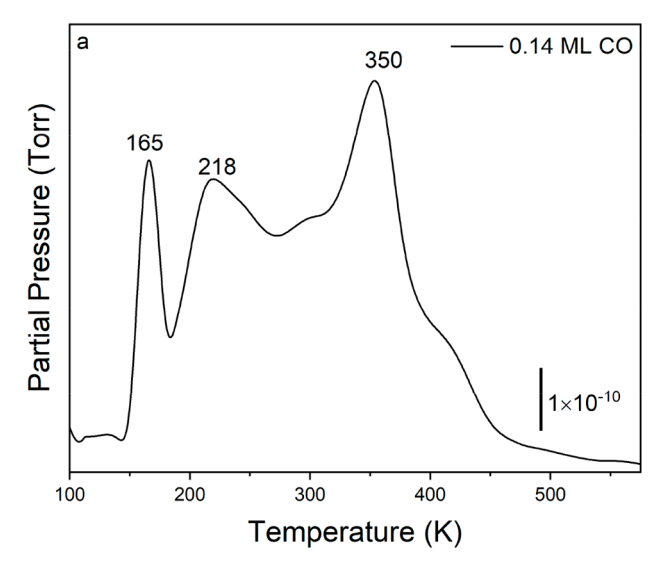
Figure 8. (a) CO TPD of a 0.45 ML Pt/Cu(111) surface showing CO desorption at 162, 220, and 352 K. The surface was saturated at 200 K (0.27 ML). (b) Room temperature RAIR spectra versus CO coverage showing the bands for CO on bridge sites (1865 cm $^{-1}$), on top of isolated Pt atoms (2050 cm $^{-1}$), and at atop sites on Pt islands (2066 cm $^{-1}$) for the 0.45 ML Pt/Cu(111) surface.

for Figure 7a. The areas obtained from peak fitting presented in the Supporting Information support this qualitative observation. The nonmonotonic change in the 162-168 K CO TPD peak area indicates changes with Pt coverage in the type of structures adopted by Pt. Identifying the Pt structures present in this coverage range could be readily accomplished through an STM study. Although Lucci et al. used STM to examine Pt structures on Cu(111), they did so only for Pt coverages ≤0.1 ML. Figure 8b shows the CO RAIR spectra of the same 0.45 ML Pt/Cu(111) surface from CO coverages of 0.024 to 0.22 ML at 300 K. The CO on Pt-Pt bridge sites is observed at 1865 cm⁻¹. For the atop CO, two peaks are observed. One grows as it shifts from 2046 to 2050 cm⁻¹, while the other shifts from 2058 to 2066 cm⁻¹ as the coverage increases. The peak at 2050 cm⁻¹ is assigned to CO on top of isolated Pt atoms, whereas the higher wavenumber peak is assigned to CO at atop sites of Pt islands. The two peaks are of roughly equal intensity for low CO coverages, but for coverages of 0.17 ML and above, the 2050 cm⁻¹ peak has reached its maximum intensity while the other peak continues to grow. This suggests that at this Pt coverage, the CO can saturate the isolated Pt atoms before it saturates the Pt islands. Like the 2050 cm⁻¹ peak, the bridge-bonded CO peak at 1865 cm⁻¹ reaches its maximum and final intensity by 0.14 ML, with no further intensity increase for higher CO coverages.

Figure 9a shows TPD of 0.14 ML of CO deposited at 200 K on a 0.23 ML Pt/Cu(111) surface. Desorption peaks for CO can be observed from Cu, mixed Cu–Pt, and Pt sites at 165, 218, and 350 K, respectively. The desorption is very similar to that of the 0.45 ML Pt/Cu(111) surface but with slightly lower peak desorption temperatures. Figure 9b shows the RAIR spectra on the same 0.23 ML Pt/Cu(111) surface for CO coverages ranging from 0.021 to 0.11 ML at 300 K. These RAIRS results follow the same trends observed with decreasing Pt coverage with the largest peak at 2047 cm⁻¹ associated with isolated Pt atoms, with CO on Pt islands giving rise to the atop peak at 2060 cm⁻¹ and a weak bridge-bonded peak at 1860 cm⁻¹.

To form the Pt/Cu(111) SAA, we deposited 0.027 ML of Pt on the Cu(111) surface at 380 K. According to the atomically resolved STM images of Lucci et al., this results in a surface in which isolated Pt atoms are substituted into the topmost atomic layer. 17 The CO TPD results in Figure 10a follow the trends seen at higher coverages of Pt deposited at room temperature with CO desorbing from Cu, mixed Cu-Pt, and Pt sites, at 168, 215, and 341 K, respectively. These CO TPD results are nearly identical with those of Lucci et al. where the CO was coadsorbed with butadiene and hydrogen on a Pt/ Cu(111) SAA. 41 Figure 10b shows the RAIR spectra of CO on the same 0.027 ML Pt/Cu(111) SAA surface at 300 K. One peak was observed at 2046 cm⁻¹, which is attributed to the adsorption of CO on top of single Pt atoms embedded in the Cu surface. A small shift from 2041 to 2046 cm⁻¹ is observed from the lowest CO coverage to saturation. Consistent with the isolated Pt atoms of the SAA, no peaks associated with CO bridge-bonding between two Pt atoms or CO adsorbed at Pt island edges or other Pt defects are observed.

Deposition of Pt at higher temperatures should produce more dispersed Pt, but also more subsurface Pt. Figure 11a shows the TPD of CO desorbing from a 0.029 ML Pt/Cu(111) SAA, where Pt was deposited at 450 K. Three distinct CO TPD peaks are again observed, but the highest temperature one due to desorption from Pt sites is more



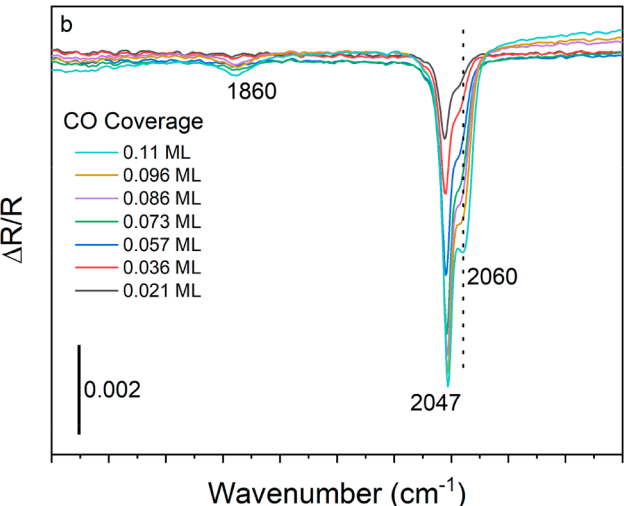


Figure 9. (a) CO TPD of a 0.23 ML Pt/Cu(111) surface showing CO desorption at 165, 218, and 350 K. The surface was saturated at 200 K (0.14 ML). (b) Room temperature RAIR spectra showing the bands for CO bridge sites (1860 cm⁻¹), on top of isolated Pt atoms (2047 cm⁻¹), and at atop sites on Pt islands (2060 cm⁻¹) for the 0.23 ML Pt/Cu(111) surface.

distinct than from the SAA prepared at 380 K. In the RAIR spectra of Figure 11b, the single peak at 2041 cm⁻¹ is sharper than observed in Figure 10b and does not shift with increasing CO coverage, suggesting the CO molecules and hence the Pt atoms are more dispersed than for the surface prepared at 380 K for the results in Figure 10.

For an even higher Pt deposition temperature of 550 K, we would expect more subsurface Pt and greater dispersal of the Pt atoms in the topmost atomic layer. The TPD results in Figure 12a are quite similar to the TPD results of Figures 10a and 11a. Like the results of Figure 11b, the RAIR spectra in Figure 12b also feature a single sharp peak at 2041 cm⁻¹ that does not shift with increasing CO coverage. For the SAA surfaces of Figures 11 and 12, the Pt atoms are evidently far enough apart that no coupling of the CO vibrations occurs.

Figure 13 shows RAIR spectra of CO on a 0.01 ML Pt/Cu(111) SAA, where the Pt was deposited at 380 K. After exposing the surface to 2 L of CO at 90 K, the black spectrum was obtained. This was followed by annealing the surface to

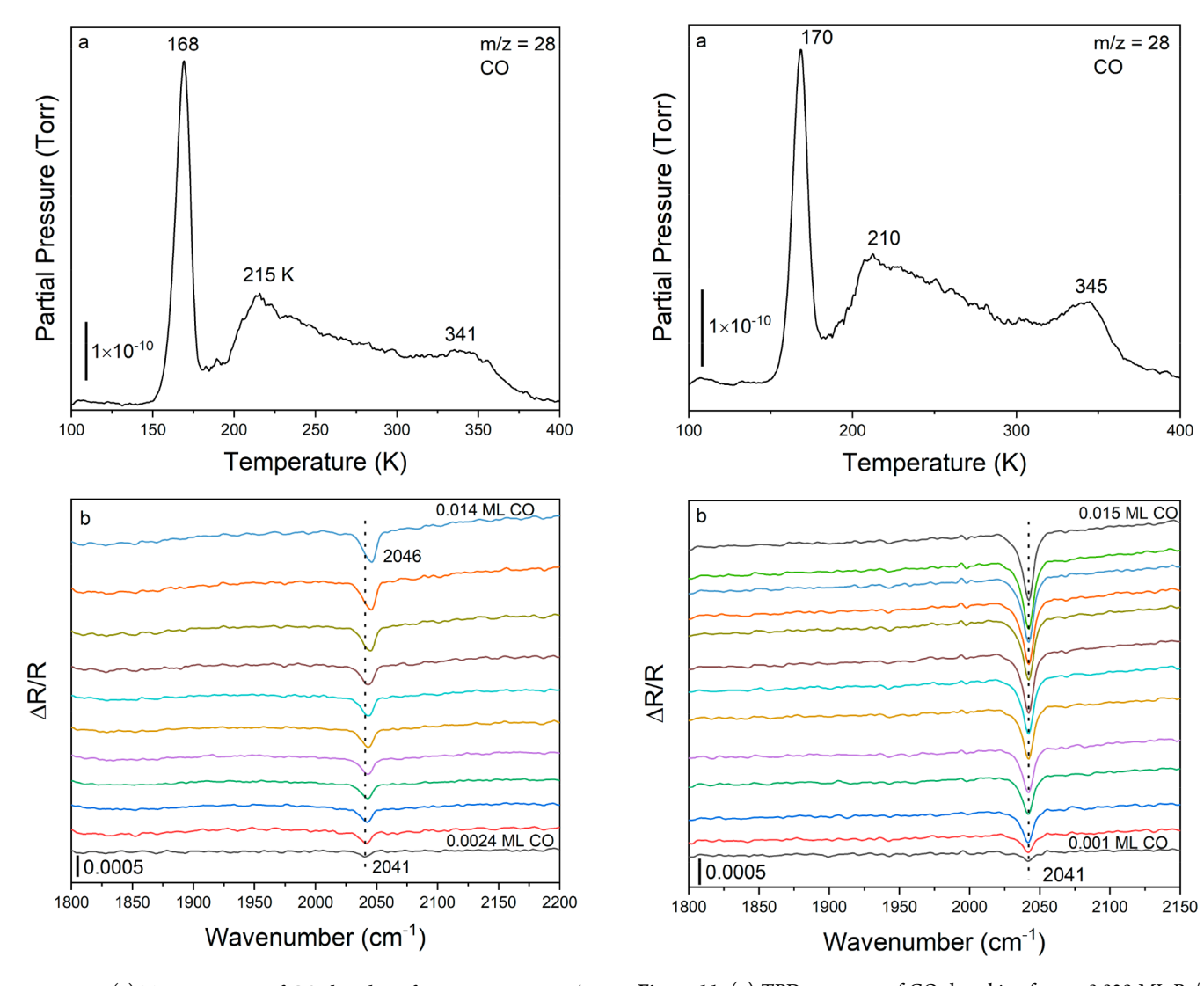


Figure 10. (a) TPD spectrum of CO desorbing from a 0.027 ML Pt/Cu(111) SAA saturated at 200 K. CO desorption from single Pt atoms occurs at 341 K. (b) Room temperature RAIR spectra of CO from the same 0.027 ML Pt/Cu(111) SAA showing the CO stretch for CO on single Pt atoms at $2041-2046 \, \mathrm{cm}^{-1}$. Pt was deposited at 380 K.

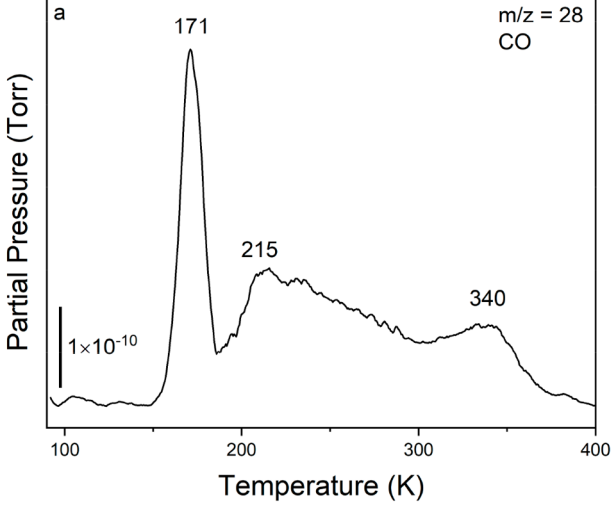
the indicated temperatures, then cooling back to 90 K where the spectra were acquired. The 2 L exposure results in a CO saturation coverage of 0.52 ML, where the peaks at 1814 and 1832, 2068, and 2130 cm⁻¹ are assigned to CO on Cu bridge sites, CO on Cu atop sites, and physisorbed CO, respectively. Annealing to 175 K (red) results in the complete loss of the Cu bridge site and physisorbed CO. A new peak is revealed at 2046 cm⁻¹, corresponding to CO on single Pt atoms on the Cu(111) surface. Further annealing to 350 K (blue) results in the loss of the peak for CO on Cu atop sites at 2078 cm⁻¹. Annealing at 400 K (green) lowers the intensity of the CO/Pt peak at 2046 cm⁻¹. After annealing to 500 K (violet), Pt diffuses into the bulk, resulting in the loss of the 2046 cm⁻¹ peak. A slight positive peak appears at this position from the presence of CO adsorbed from the background when the reference spectrum was obtained. After the 500 K anneal, the surface was exposed to 0.5 L of CO at 90 K and then annealed to 175 K. This yields a small peak at 2078 cm⁻¹ due to a small amount of CO on Cu atop sites. The fact that the 2046 cm⁻¹

Figure 11. (a) TPD spectrum of CO desorbing from a 0.029 ML Pt/Cu(111) SAA saturated at 200 K. CO desorption from single Pt atoms occurs at 345 K. (b) Room temperature RAIR spectra of CO from the same 0.029 ML Pt/Cu(111) SAA showing the CO stretch for CO on single Pt atoms at 2041 cm $^{-1}$. Pt was deposited at 450 K.

does not reappear demonstrates that the CO does not cause Pt to segregate back to the surface under these conditions.

4. DISCUSSION

The IR spectra of CO adsorbed on Pt/Cu(111) reported here provide new insights into this extensively studied bimetallic surface. The previous results indicating that Pt grows layer-bylayer on Cu(111) implies that a monolayer of Pt would have the same hexagonal surface lattice and lattice constant as that of Cu(111), implying a pseudomorphic Pt layer compressed by 7% relative to a Pt(111) surface. Additional layers were found to grow epitaxially and to assume the Pt lattice constant by 5 Pt layers. Like Pt(111), our RAIRS results for the multilayer Pt film show the initial occupation of Pt atop sites followed by bridge sites, corresponding to CO peaks at 2089 and 1862 cm⁻¹ at saturation coverage, presumed to be 0.5 ML. Although the lowest coverage position of the atop peak is difficult to determine because of the adsorption of background CO, there is a total shift of at least +20 cm⁻¹. This shift can be compared with what has been reported for CO on Pt(111), where



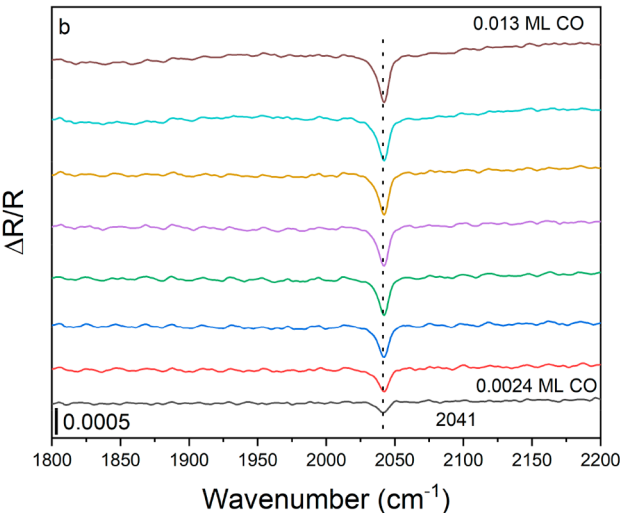


Figure 12. (a) TPD spectrum of CO desorbing from a 0.026 ML Pt/Cu(111) SAA saturated at 200 K. CO desorption from single Pt atoms occurs at 340 K. (b) Room temperature RAIR spectra of CO from the same 0.026 ML Pt/Cu(111) SAA showing the CO stretch from CO on single Pt atoms at 2041 cm $^{-1}$. Pt was deposited at 550 K.

isotopic dilution experiments, either \$^{12}C^{16}O/^{12}C^{18}O\$ (refs 20 and 22) or ¹²C¹⁶O/¹³C¹⁶O (ref 21) were used to distinguish dipole-coupling shifts from chemical shifts. For example, Olsen and Masel showed that the atop CO peak shifts from 2084 cm⁻¹ at the lowest coverage to 2095 cm⁻¹ at 0.5 ML at 300 K and that this 11 cm⁻¹ shift consisted of a +25 cm⁻¹ coupling shift combined with a -14 cm⁻¹ chemical shift. Tüshaus et al. reported that the atop peak shifts from 2089 to 2103 cm⁻¹ from the lowest coverages to 0.5 ML, with the bridge species at about 1852 cm⁻¹ at 0.5 ML, with little change in position with coverage.²⁰ They also concluded that the total shift at 0.5 ML consisted of a large positive coupling shift partially offset by a smaller negative chemical shift. Our observed shift of at least +20 cm⁻¹ is notably larger than observed on Pt(111). Since the coupling shift is likely to be the same for the Pt monolayer and for Pt(111), the comparison implies a much smaller red-shift due to the bonding interaction with the surface (the chemical shift) for Pt/Cu(111), although confirmation of this would require isotopic dilution experiments. Regardless of the exact composition of the coverage-dependent shift, the strongly red-

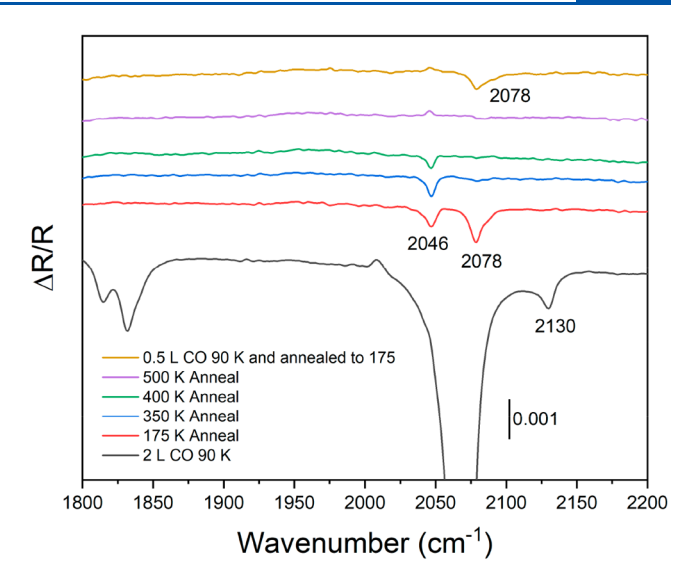


Figure 13. RAIR spectra of a 0.01 ML Pt/Cu(111) SAA prepared by depositing Pt at 380 K and after exposure to 2 L of CO at 90 K. The surface was then annealed to 175, 350, 400, and 500 K (red, blue, green, and purple spectra, respectively). After the 500 K anneal, the surface was exposed to 0.5 L of CO and annealed to 175 K (gold spectrum).

shifted C–O stretch frequency in the limit of zero CO coverage on the Pt/Cu(111) multilayer film surface compared to CO on Pt(111) reveals that the Pt atoms of the pseudomorphic Pt layer on Cu(111) are chemically distinct from the Pt atoms of a Pt(111) surface. A similar conclusion was reached by Fusy et al. based on CO TPD and PAX results. 13

At the other extreme of Pt coverages are the SAA surfaces. Low coverages of Pt deposited at 380, 450, and 550 K give rise to a single C-O stretch peak in the range of 2041 to 2046 cm⁻¹. The absence of a bridge-bonded peak is consistent with the presence of only isolated Pt atoms in the Cu(111) surface layer. For the 380 K Pt deposition, there is a small shift from 2041 to 2046 cm⁻¹ as the CO coverage increases, but there is no detectable shift for the 450 and 550 K Pt depositions. This is consistent with the STM observations of Lucci et al. that for lower deposition temperatures the Pt tends to accumulate near the step edges where it would have a higher areal density, whereas for depositions at 450 and 550 K, the Pt atoms are well dispersed within the Cu(111) terraces. 16 The nature of the bonding between CO and the Pt atoms of the SAA surfaces is revealed to be different from the bonding between CO and a Pt atom of Pt(111) by the low value of the C–O stretch, which is a sensitive indicator of charge transfer between the metal surface and the CO molecular orbitals. In the limit of zero coverage, the C-O stretch on Pt(111) occurs at 2084-2089 cm⁻¹, indicating that a Pt atom surrounded by Cu atoms is electronically distinct from a Pt atom surrounded by other Pt atoms. This is consistent with the density functional theory (DFT) calculations of Darby et al., who found that the CO binding energy on the Pt atom of a Pt/Cu(111) SAA was -1.18 eV compared to -1.48 on Pt(111). In contrast to our results for the Pt/Cu(111) SAA where the C-O stretch of CO on the isolated Pt atoms occurs in the range of 2041-2050 cm⁻¹, Liu et al. reported that CO adsorbed on the Pt sites of an Al₂O₃-supported Pt_{0.008}Cu SAA nanocatalyst had a substantially higher C-O stretch value of 2088 cm^{-1,32} Their C-O

stretch frequencies of CO adsorbed on Cu and Pt aggregate sites were also significantly different from the values we report for CO on the analogous sites of Pt/Cu(111). The differences indicate that the bonding properties of the corresponding sites of the single crystal surfaces and the nanocatalysts do not have identical chemical properties.

The interpretation of the IR spectra for the Pt multilayer and Pt/Cu(111) SAAs provides a firm basis for interpreting the CO spectra for intermediate Pt coverages. After depositing 0.62, 0.45, and 0.23 ML of Pt at 300 K, the atop C-O stretch shows two components, with the lower frequency component in the range of 2047-2050 cm⁻¹ and the higher frequency component in the range of 2058-2067 cm⁻¹. The decrease with decreasing Pt coverage of the 2058-2067 cm⁻¹ peak and the presence of the bridge-bonded CO only when the higher frequency atop CO peak is observed implies that this peak is associated with small Pt-containing islands, with the 2047-2050 cm⁻¹ peak due to isolated Pt atoms in the terraces. The lack of a significant blue-shift of the peak for CO on atop sites of the Pt islands suggests that they are small and well separated. On a small island, there are not enough CO molecules to produce the full coupling shift and the islands are too well separated for coupling to occur between molecules on different islands. Confirmation of these indirect inferences about the distribution of Pt islands at higher Pt coverages would require study with a direct structural probe such as STM.

The CO IR spectra for intermediate Pt coverages are surprisingly simple given the complicated nature of the structures observed by Lucci et al. for Pt deposited on Cu(111) at 315 K for Pt coverages of 0.01 and 0.1 ML. 16 For the higher Pt coverage, they observed both well dispersed Pt in the Cu(111) terraces as well as Pt-rich brims and fingers at the step edges. Furthermore, they observed in some cases that the fingers contained both Pt and Cu atoms in locally ordered p(2 \times 2) and ($\sqrt{3} \times \sqrt{3}$)-R 30° structures with Cu₃Pt and Cu₂Pt stoichiometries. They also showed that islands contained both Cu and Pt, with the Pt concentrated near the island edges. If such structures were also present at the Pt coverages studied here, then the 2060-2067 cm⁻¹ peak could be reasonably assigned to CO at Pt atop sites of these Cu₃Pt and Cu₂Pt structures, rather than to atop sites of pure Pt islands. However, the observation of bridge-site CO implies that there are at least some islands containing adjacent Pt atoms, an arrangement that is not present in the p(2 \times 2) and ($\sqrt{3}$ \times $\sqrt{3}$)-R 30° structures observed by Lucci et al. ¹⁶ Although the STM images reveal a variety of different environments for the Pt atoms, each of these environments do not give rise to a detectably different C-O stretch frequency. Instead, it appears that the RAIRS spectrum of CO on the Pt/Cu(111) surface only allows distinction between isolated Pt atoms surrounded by Cu atoms, or Pt atoms that are part of islands, either pure Pt islands or mixed Pt-Cu islands.

5. CONCLUSIONS

The adsorption of CO on Pt deposited onto a Cu(111) surface provides new insights into the properties of this bimetallic surface. In accord with several past studies, TPD of CO shows distinct desorption peaks due to adsorption on Cu, mixed Cu—Pt sites, and Pt sites. Previous studies have shown that a monolayer of Pt adopts a pseudomorphic structure with the Pt atoms occupying fcc hollow sites on the Cu surface, such that the Pt—Pt distances are the same as the Cu—Cu distances. The

Pt monolayer on Cu(111) is thus compressed by 7% relative to the Pt-Pt distance of the Pt(111) surface. Whether due to compressive stress or Pt-Cu charge transfer, the C-O stretch of CO adsorbed on the pseudomorphic Pt layer is red-shifted relative to its value on Pt(111). As the Pt coverage decreases, the presence of isolated Pt atoms in the Cu(111) terraces is revealed by the appearance of a C-O stretch peak in the range of 2041-2050 cm⁻¹, while the presence of Pt islands is revealed by a peak due to atop CO in the range of 2058-2067 cm⁻¹, which is always accompanied by a C-O stretch peak at 1862-1870 cm⁻¹ due to CO bridge-bonded between two Pt atoms. The formation of a SAA is readily revealed by a C-O stretch peak at 2041 cm⁻¹ that does not shift with increasing CO coverage and that is unaccompanied by a C-O stretch due to bridge-bonded CO. The significant red-shift of the C-O stretch for CO on the Pt atoms of the SAA relative to the C-O stretch of CO in the limit of zero coverage on Pt(111) reveals how the properties of a Pt atom surrounded by Cu atoms is altered relative to those of a Pt atom surrounded by other Pt atoms. This implies that the catalytic properties of the Pt atoms of the Pt/Cu(11) SAA may be distinctly different from those of pure Pt catalysts.

ASSOCIATED CONTENT

Supporting Information

The Supporting Information is available free of charge at https://pubs.acs.org/doi/10.1021/acs.jpcc.3c00896.

Peak fitting results for the CO TPD traces for each Pt coverage and a plot of CO peak areas versus Pt coverage (PDF)

AUTHOR INFORMATION

Corresponding Author

Michael Trenary — Department of Chemistry, University of Illinois Chicago, Chicago, Illinois 60607, United States; orcid.org/0000-0003-1419-9252; Email: mtrenary@uic.edu

Authors

David L. Molina — Department of Chemistry, University of Illinois Chicago, Chicago, Illinois 60607, United States; orcid.org/0000-0002-0580-8442

Maki Inagaki — Department of Applied Chemistry, School of Engineering, The University of Tokyo, Tokyo 113-8656, Japan; orcid.org/0000-0002-8876-320X

Emiko Kazuma — Department of Applied Chemistry, School of Engineering, The University of Tokyo, Tokyo 113-8656, Japan; orcid.org/0000-0003-0834-9832

Yousoo Kim — Surface and Interface Science Laboratory, RIKEN, Wako, Saitama 351-0198, Japan; Department of Applied Chemistry, School of Engineering, The University of Tokyo, Tokyo 113-8656, Japan; orcid.org/0000-0001-7730-0704

Complete contact information is available at: https://pubs.acs.org/10.1021/acs.jpcc.3c00896

Notes

The authors declare no competing financial interest.

ACKNOWLEDGMENTS

We gratefully acknowledge financial support from the National Science Foundation (CHE-2102622).

REFERENCES

- (1) Chen, J. G.; Menning, C. A.; Zellner, M. B. Monolayer bimetallic surfaces: Experimental and theoretical studies of trends in electronic and chemical properties. *Surf. Sci. Rep.* **2008**, *63*, 201–254.
- (2) Rodriguez, J. A. Physical and chemical properties of bimetallic surfaces. *Surf. Sci. Rep.* **1996**, *24*, 223–287.
- (3) Castro, G. R.; Schneider, U.; Busse, H.; Janssens, T.; Wandelt, K. The interaction of CO with the $Cu_3Pt(111)$ surface. *Surf. Sci.* **1992**, 269–270, 321–325.
- (4) Shen, Y. G.; O'Connor, D. J.; Wandelt, K.; MacDonald, R. J. Studies of surface composition and structure of Cu₃Pt(111) by low energy alkali ion scattering. *Surf. Sci.* **1995**, 328, 21–31.
- (5) Sheppard, N.; De La Cruz, C. The reliability of vibrational spectroscopy as a means of identification of the structures of chemisorbed species on metal surfaces: the cases of CO, NO and C₂ hydrocarbon surface species. *Catal. Today* **2001**, *70*, 3–13.
- (6) Hannagan, R. T.; Giannakakis, G.; Flytzani-Stephanopoulos, M.; Sykes, E. C. H. Single-Atom Alloy Catalysis. *Chem. Rev.* **2020**, *120*, 12044–12088.
- (7) Kruppe, C. M.; Krooswyk, J. D.; Trenary, M. Polarization-Dependent Infrared Spectroscopy of Adsorbed Carbon Monoxide To Probe the Surface of a Pd/Cu(111) Single-Atom Alloy. *J. Phys. Chem.* C 2017, 121, 9361–9369.
- (8) Hannagan, R. T.; Patel, D. A.; Cramer, L. A.; Schilling, A. C.; Ryan, P. T. P.; Larson, A. M.; Çınar, V.; Wang, Y.; Balema, T. A.; Sykes, E. C. H. Combining STM, RAIRS and TPD to Decipher the Dispersion and Interactions Between Active Sites in RhCu Single-Atom Alloys. *ChemCatChem.* **2020**, *12*, 488–493.
- (9) Muir, M.; Trenary, M. Adsorption of CO to Characterize the Structure of a Pd/Ag(111) Single-Atom Alloy Surface. *J. Phys. Chem.* C **2020**, *124*, 14722–14729.
- (10) Belkhou, R.; Barrett, N. T.; Guillot, C.; Barbier, A.; Eugène, J.; Carrière, B.; Naumovic, D.; Osterwalder, J. Growth of Pt/Cu(111) characterised by Auger electron spectroscopy, core level photoemission and X-ray photoelectron diffraction. *Appl. Surf. Sci.* 1993, 65–66, 63–70.
- (11) Shen, Y. G.; O'Connor, D. J.; Wandelt, K.; MacDonald, R. J. Thin film growth of Pt on Cu(111): a LEIS study. *Surf. Sci.* **1996**, 357–358, 921–925.
- (12) Miszczuk, A.; Morawski, I.; Jurczyszyn, M.; Nowicki, M. Properties of Pt on Cu(111) revealed by AES, LEED, and DEPES. *J. Electron. Spec. Rel. Phen.* **2018**, 223, 29–36.
- (13) Fusy, J.; Menaucourt, J.; Alnot, M.; Huguet, C.; Ehrhardt, J. J. Growth and reactivity of evaporated platinum films on Cu(111): a study by AES, RHEED and adsorption of carbon monoxide and xenon. *Appl. Surf. Sci.* **1996**, *93*, 211–220.
- (14) Belkhou, R.; Barrett, N. T.; Guillot, C.; Fang, M.; Barbier, A.; Eugène, J.; Carrière, B.; Naumovic, D.; Osterwalder, J. Formation of a surface alloy by annealing of Pt/Cu(111). *Surf. Sci.* **1993**, *297*, 40–56.
- (15) Schröder, U.; Linke, R.; Boo, J. H.; Wandelt, K. Adsorption properties and formation of PtCu surface alloys. *Surf. Sci.* **1996**, 352–354, 211–217.
- (16) Lucci, F. R.; Lawton, T. J.; Pronschinske, A.; Sykes, E. C. H. Atomic Scale Surface Structure of Pt/Cu(111) Surface Alloys. *J. Phys. Chem. C* **2014**, *118*, 3015–3022.
- (17) Lucci, F. R.; Marcinkowski, M. D.; Lawton, T. J.; Sykes, E. C. H. H₂ Activation and Spillover on Catalytically Relevant Pt-Cu Single Atom Alloys. *J. Phys. Chem. C* **2015**, *119*, 24351–24357.
- (18) Hollins, P.; Pritchard, J. Interactions of CO molecules adsorbed on Cu(111). Surf. Sci. 1979, 89, 486–495.
- (19) Persson, B. N. J.; Liebsch, A. Collective vibrational modes of isotopic mixtures of CO on Cu(111) and Cu(001). *Surf. Sci.* **1981**, 110, 356–368.
- (20) Tüshaus, M.; Schweizer, E.; Hollins, P.; Bradshaw, A. M. Yet another vibrational study of the adsorption system platinum{111}-carbon monoxide. *J. Electron. Spec. Rel. Phen.* 1987, 44, 305–16.
- (21) Olsen, C. W.; Masel, R. I. An infrared study of CO adsorbed on Pt(111). Surf. Sci. 1988, 201, 444.

- (22) Schweizer, E.; Persson, B. N. J.; Tüshaus, M.; Hoge, D.; Bradshaw, A. M. The potential energy surface, vibrational phase relaxation and the order-disorder transition in the adsorption system platinum{111}-carbon monoxide. *Surf. Sci.* **1989**, 213, 49–89.
- (23) Reutt-Robey, J. E.; Doren, D. J.; Chabal, Y. J.; Christman, S. B. Microscopic CO Diffusion on a Pt(111) Surface by Time-Resolved Infrared Spectroscopy. *Phys. Rev. Lett.* **1988**, *61*, 2778–2781.
- (24) Agrawal, V. K.; Trenary, M. An Infrared Study of NO Adsorption at Defect Sites on Pt(111). Surf. Sci. 1991, 259, 116–128. (25) Hayden, B. E.; Bradshaw, A. M. The adsorption of CO on Pt(111) studied by infrared reflection-absorption spectroscopy. Surf. Sci. 1983, 125, 787–802.
- (26) Malik, I. J.; Trenary, M. Infrared Reflection Absorption Study of the Adsorbate Substrate Stretch of CO on Pt(111). *Surf. Sci.* **1989**, 214, L237–L245.
- (27) Ryberg, R. Phase transitions in a chemisorbed overlayer studied by infrared spectroscopy: CO on Pt(111). *Phys. Rev. B* **1989**, *40*, 865–868.
- (28) Yang, H. J.; Minato, T.; Kawai, M.; Kim, Y. STM Investigation of CO Ordering on Pt(111): From an Isolated Molecule to High-Coverage Superstructures. J. Phys. Chem. C 2013, 117, 16429–16437.
- (29) Ertl, G.; Neumann, M.; Streit, K. M. Chemisorption of CO on the Pt(111) surface. Surf. Sci. 1977, 64, 393-410.
- (30) Kirstein, W.; Krüger, B.; Thieme, F. CO adsorption studies on pure and Ni-covered Cu(111) surfaces. Surf. Sci. 1986, 176, 505–529.
- (31) Darby, M. T.; Sykes, E. C. H.; Michaelides, A.; Stamatakis, M. Carbon Monoxide Poisoning Resistance and Structural Stability of Single Atom Alloys. *Top. Catal.* **2018**, *61*, 428–438.
- (32) Liu, J. L.; Lucci, F. R.; Yang, M.; Lee, S.; Marcinkowski, M. D.; Therrien, A. J.; Williams, C. T.; Sykes, E. C. H.; Flytzani-Stephanopoulos, M. Tackling CO Poisoning with Single-Atom Alloy Catalysts. J. Am. Chem. Soc. 2016, 138, 6396–6399.
- (33) Hayden, B. E.; Kretzschmar, K.; Bradshaw, A. M. An infrared spectroscopic study of CO on Cu(111): The linear, bridging and physisorbed species. *Surf. Sci.* 1985, 155, 553–566.
- (34) Raval, R.; Parker, S. F.; Pemble, M. E.; Hollins, P.; Pritchard, J.; Chesters, M. A. FT-RAIRS, EELS, and LEED Studies of the Adsorption of Carbon Monoxide on Cu(111). *Surf. Sci.* **1988**, *203*, 353–377.
- (35) Eve, J. K.; McCash, E. M. Low-temperature adsorption of CO on Cu(111) studied by reflection absorption infrared spectroscopy. *Chem. Phys. Lett.* **1999**, 313, 575–581.
- (36) Eve, J. K.; McCash, E. M. Low-temperature adsorption of CO on Cu(111) studied by RAIRS. *Chem. Phys. Lett.* **2002**, 360, 202–208
- (37) McCabe, R. W.; Schmidt, L. D. Binding states of CO and H_2 on clean and oxidized (111)Pt. Surf. Sci. 1977, 65, 189–209.
- (38) Gorte, R. J.; Schmidt, L. D. Interactions between NO and CO on Pt(111). Surf. Sci. 1981, 111, 260–278.
- (39) Hollins, P.; Pritchard, J. Infrared Studies of Chemisorbed Layers on Single Crystals. *Prog. Surf. Sci.* **1985**, *19*, 275–349.
- (40) Simonovis, J. P.; Hunt, A.; Palomino, R. M.; Senanayake, S. D.; Waluyo, I. Enhanced Stability of Pt-Cu Single-Atom Alloy Catalysts: In Situ Characterization of the Pt/Cu(111) Surface in an Ambient Pressure of CO. *J. Phys. Chem. C* **2018**, *122*, 4488–4495.
- (41) Lucci, F. R.; Liu, J. L.; Marcinkowski, M. D.; Yang, M.; Allard, L. F.; Flytzani-Stephanopoulos, M.; Sykes, E. C. H. Selective hydrogenation of 1,3-butadiene on platinum-copper alloys at the single-atom limit. *Nat. Commun.* **2015**, *6*, 8550–8556.